

Cite this: *Phys. Chem. Chem. Phys.*, 2012, **14**, 16612–16617

www.rsc.org/pccp

PAPER

Searching for active binary rutile oxide catalyst for water splitting from first principles†‡

Dong Chen, Ya-Hui Fang and Zhi-Pan Liu*

Received 27th June 2012, Accepted 2nd August 2012

DOI: 10.1039/c2cp42149f

Water electrolysis is an important route to large-scale hydrogen production using renewable energy, in which the oxygen evolution reaction (OER: $2\text{H}_2\text{O} \rightarrow \text{O}_2 + 4\text{H}^+ + 4\text{e}^-$) causes the largest energy loss in traditional electrocatalysts involving Ru–Ir mixed oxides. Following our previous mechanistic studies on the OER on $\text{RuO}_2(110)$ (*J. Am. Chem. Soc.* 2010, **132**, 18214), this work aims to provide further insight into the key parameters relevant to the activity of OER catalysts by investigating a group of rutile-type binary metal oxides, including RuNiO_2 , RuCoO_2 , RuRhO_2 , RuIrO_2 and OsIrO_2 . Two key aspects are focused on, namely the surface O coverage at the relevant potential conditions and the kinetics of H_2O activation on the O-covered surfaces. The O coverage for all the oxides investigated here is found to be 1 ML at the concerned potential (1.23 V) with all the exposed metal cations being covered by terminal O atoms. The calculated free energy barrier for the H_2O dissociation on the O covered surfaces varies significantly on different surfaces. The highest OER activity occurs at RuCoO_2 and RuNiO_2 oxides with a predicted activity about 500 times higher than pure RuO_2 . On these oxides, the surface bridging O near the terminal O atom has a high activity for accepting the H during H_2O splitting. It is concluded that while the differential adsorption energy of the terminal O atom influences the OER activity to the largest extent, the OER activity can still be tuned by modifying the electronic structure of surface bridging O.

1. Introduction

Electrochemical water splitting is an attractive route to clean hydrogen production and thus has raised tremendous interest in recent years.^{1–8} The overall process can be divided into two half-cell redox reactions,⁹ the hydrogen evolution reaction (HER): $2\text{H}^+ + 2\text{e}^- \rightarrow \text{H}_2$ and oxygen evolution reaction (OER): $\text{H}_2\text{O} \rightarrow \frac{1}{2}\text{O}_2 + 2\text{H}^+ + 2\text{e}^-$. Because the OER at the anode suffers from a substantial energy loss owing to the high overpotential (~ 0.3 V) on traditional catalysts (RuO_2 , IrO_2 mixed oxides^{3,10}), huge efforts have been devoted to search for better OER catalysts by means of experimental and theoretical approaches.^{9–17} Recently, a large number of bimetal OER catalysts has been synthesized and investigated by doping a second metal into the RuO_2 catalyst, including Ru–Ir,^{3,10,11} Ru–Co,^{10,15,18,19} Ru–Ni,^{5,10,13} Ru–Re,¹⁰ Ru–Pt,²⁰ Ru–Cu,¹⁰ Ru–Ce,^{15,21} Ru–Pb,^{22,23} Ru–Cr,^{10,24} Ru–Fe²⁵ and Ru–W.²⁶

Among them, Ni and Co doped RuO_2 catalysts are shown to increase the activity while the Ir doped RuO_2 catalyst lowers the activity but improves the catalyst stability. To improve systematically the performance of OER catalysts, achieving a better understanding for OER on the doped oxide systems and identify the key parameters that are relevant to the activity are essential steps. An interesting question raised is therefore whether the activity of the doped oxide systems can be predicted from theory by properly taking into account the complex reaction conditions, *i.e.* at the solid–liquid interface under electrochemical conditions.

Apart from the experimental trial-and-error search for better OER catalysts, recent years have also seen theoretical attempts to understand the OER mechanism, in particular, on rutile oxide (110) surfaces. Using a thermodynamics approach, the Nørskov group^{7,8,27,28} first showed that the binding strength of the O-containing intermediates (OH, O, OOH) is important to electrocatalytic activity. By correlating the experimental measured OER activity with the DFT calculated atomic O binding energy, they suggested that the O binding strength should neither be too strong nor too weak.²⁸ Although a simplified thermodynamics model was utilized in the work (*e.g.* without explicitly considering the electrochemical environment such as potential and solvation), these theoretical results undoubtedly provide valuable insights into the fundamental

Shanghai Key Laboratory of Molecular Catalysis and Innovative Materials, Department of Chemistry, Key Laboratory of Computational Physical Science (Ministry of Education), Fudan University, Shanghai 200433, China. E-mail: zpliu@fudan.edu.cn

† Electronic supplementary information (ESI) available. See DOI: 10.1039/c2cp42149f

‡ This article was submitted as part of a collection on Computational Catalysis and Materials for Energy Production, Storage and Utilization.

quantities in dictating the OER activity. By focusing on the reaction kinetics with the DFT-based periodic continuum solvation model, our group¹² recently investigated the OER on rutile RuO_2 (110) under the electrochemical environment and a complete atomic-level mechanism for OER was revealed. It showed that water oxidation initially follows an Eley–Rideal-like mechanism, where the breaking of the HO–H bond on the O-terminated (110) facet is the rate-determining step with the terminal O atom accepting the OH and the lattice bridging O atom accepting the H. Because the terminal O atom directly takes part in H_2O activation, it was suggested that the differential adsorption energy of the terminal O atom, defined as $\delta G(\text{O})$, on the surface at the concerned potential dictates the OER activity. A -0.7 to 0 eV energy window for $\delta G(\text{O})$ at ~ 1.23 V is expected for any good OER catalyst.

For the purpose of the rational design of new OER catalysts, it is intriguing to further apply the above-identified models/quantities, such as the $\delta G(\text{O})$, to understand and even predict the activity of any proposed catalyst and compare the theoretical rate with the experimental value, if available. Since rutile-type binary metal oxides have been heavily investigated experimentally, this work investigates five different rutile-type binary metal oxide systems with first principles calculations. Two key questions are focused on: (i) what is the theoretical overpotential for these binary metal oxide catalysts and (ii) can the OER activity be correlated with the $\delta G(\text{O})$? Both the *in situ* surface coverage (thermodynamics) of these systems and the reaction barrier of H_2O initial bond breaking (kinetics) are calculated to predict the OER catalytic activity. We show that the reaction barrier can be remarkably reduced by mixing RuO_2 with 3d and 4d late-transition metal elements (X), such as Ni, Co and Rh, to form RuXO_2 binary oxides. By analyzing the surface electronic structure and correlating the reactivity with $\delta G(\text{O})$, we conclude that RuCoO_2 is a potential OER catalyst with good activity and reasonable stability.

2. Methods and models

For the fast screening of different catalysts at the same theoretical level, in this work we utilize the standard periodic density functional theory method with plane wave basis set²⁹ at the exchange-correlation level of GGA-PBE.³⁰ Spin-polarized calculations have been performed for the materials involving 3d/4d cationic atoms. The other DFT calculation setup has been described in our previous work.³¹ All the transition states (TS) of H_2O dissociation on different surfaces were searched using constrained-Broyden-minimization³² and constrained-Broyden-Dimer method.³³

Five rutile-type binary ABO_2 oxides (*i.e.* mole ratio A : B = 1 : 1), namely, RuNiO_2 , RuCoO_2 , RuRhO_2 , RuIrO_2 and OsIrO_2 are selected as the model systems for comparing the OER activity with pure RuO_2 . The lattice of these oxides was first determined through the optimization of the lattice constant while fixing the rutile lattice symmetry. The calculated lattice constants ($a = b, c$, unit Å) for these oxides are RuNiO_2 : (4.430, 3.065); RuCoO_2 : (4.435, 3.022); RuO_2 : (4.521, 3.116); RuRhO_2 : (4.594, 3.147); RuIrO_2 : (4.583, 3.182) and OsIrO_2 : (4.584, 3.219), respectively.

Because pure DFT functionals have a well-known deficiency in calculating the electronic structure of strong-correlation

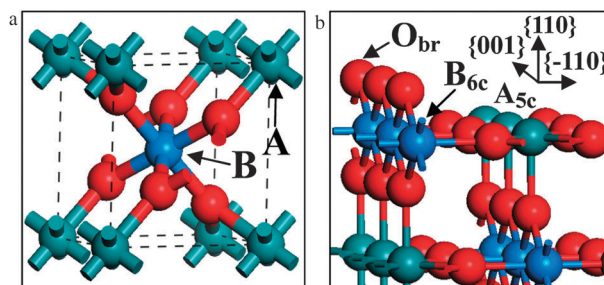


Fig. 1 The bulk structure of the rutile-type binary ABO_2 oxide (a) and its (110) surface with A cations exposed as five-coordinated sites (b).

systems, we have examined our results involving 3d cations using the GGA + U approach.³⁴ Specifically, for Ni and Co doped RuO_2 systems, the U value utilized is 3.5 eV and 3 eV for the 3d orbital of Ni and Co, respectively. It is intriguing to find that the RuNiO_2 and RuCoO_2 model systems are always metallic systems with and without the plus-U approach (the calculated total density of states are shown in the ESI†, Fig. S-1). This is due to the fact that RuO_2 is a metallic system and the Ni/Co doped systems still maintain a large number of Ru–O bondings. In general, we found that the effect of U to the calculated adsorption energy is rather small (*i.e.* < 0.1 eV), as shown in the ESI†, Table S-1.

The (110) surface, the most stable facet of rutile structure, is considered as the model surface for OER. For the binary ABO_2 oxides, there are two possible surface terminations distinguishable by which element is exposed as the five-coordinated sites (see Fig. 1b). In this work, we are interested in the possible catalytic role of the other dopants that are added into RuO_2 . Therefore, we only considered the termination with Ru being exposed as the five-coordinated sites for RuNiO_2 , RuCoO_2 , RuRhO_2 and RuIrO_2 binary oxides. We also considered replacing Ru as Os, the 5d analogue of Ru (beneath Ru in the periodic table), and studied the OsIrO_2 binary oxide with Os being exposed as the five-coordinated site. It should be mentioned that the exact structure of these binary oxides remains unclear in experiment¹⁰ and therefore the study presented here is a theoretical survey focusing on the catalytic role of dopants as the electronic structure modifier without considering the structural reconstruction due to the dopant. Similar to our previous work on RuO_2 , a six-layer oxide slab has been utilized for all calculations.¹² We have examined the convergence of slab thickness on the adsorption of O atom, which shows that the adsorption energy of the O atom (1 ML) on RuO_2 (110) is -0.60 , -0.64 and -0.62 eV at 6, 8 and 10 layer slabs, respectively. On all relaxed clean (110) surfaces, the surface shows the typical rumpling with the exposed five-fold metal cations (cation A) moving towards the bulk and the shortening of the bond length between the bridging O and the six-fold metal cation (cation B).

3. Results

Recent advances in theoretical modeling have demonstrated that it is now possible from first principles to understand the kinetics of electrochemical reactions provided with the knowledge of the detailed catalyst surface structure.^{12,31,35} This can be done by

exhaustive exploration of all the likely reaction pathways under the electrochemical conditions. For the purpose of the catalyst screening, such first principles simulations are still too computationally demanding and are in fact not worthwhile because the accurate description of kinetics on obviously poor catalysts will dominate the computational cost. In this work, we will mainly focus on two key aspects that are known to be important for OER activity as learned from our previous work on the RuO₂(110) surface.¹² They are (i) the surface coverage of O atoms and (ii) the kinetics for H₂O dissociation on the relevant O-covered (110) surfaces. By comparing the DFT calculated rate with experimental data,¹⁰ we will show that this simplified approach could be utilized as a practical tool for the fast screening of OER catalyst.

As OER occurs above 1.23 V, H₂O in solution will dissociate into O atoms that can adsorb on the surface, leading to a variety of O-containing phases. The coverage of surface O atoms therefore needs to be determined for the investigation of OER. By gradually adding O atoms onto the (110) surfaces of RuO₂ and five rutile-type binary metal oxides, we have considered different surface coverage conditions, including 1/3 ML, 2/3 ML, 1 ML, 4/3 ML (Fig. 2b). Below 1 ML, the O atoms will gradually occupy the exposed five-fold metal cationic site, forming the terminal O; above 1 ML, as the surface is already fully O-exposed, the additional O atoms have to bond with the terminal O atoms, forming adsorbed terminal O₂. The $\delta G(O)$ can be calculated using eqn (1) with

respect to molecular O₂ at the standard state (equivalent to H₂O/H⁺ in solution at 1.23 V and standard state) and all the results are plotted in Fig. 2a.

$$\delta G(O) = G(S-O) - G(S) - 1/2G(O_2) \quad (1)$$

where G(S) and G(S-O) represent the Gibbs free energy for the surface before and after adsorbing an additional amount of O (it is 1/3 ML in this work due to the finite unit cell utilized). Fig. 2 shows that 1 ML O coverage is thermodynamically stable with $\delta G(O)$ being negative for all the surfaces at 1.23 V. Further increasing the O atom coverage to 4/3 ML, the O atom becomes unstable compared to molecular O₂. The computed $\delta G(O)$ above 1 ML is generally positive, indicating that these high O coverages are only achievable at potentials substantially higher than 1.23 V. Since we are concerned with a low overpotential OER catalyst, the 1 ML O coverage surface condition is therefore the most relevant surface composition in order to assess the activity of the catalyst.

For the 1 ML O-covered surface, all the oxides investigated exhibit a similar bond distance between the terminal O atom and the five-fold A cation, ranging from 1.70 to 1.72 Å. Although the bond distance is almost identical, $\delta G(O)$ is not the same: at the 1 ML O-covered surface, $\delta G(O)$ is -0.48 eV, -0.50 eV, -0.60 eV, -0.75 eV, -0.95 eV and -2.26 eV on the RuNiO₂, RuCoO₂, RuO₂, RuRhO₂, RuIrO₂ and OsIrO₂ surfaces, respectively. Our calculations show that the 5d-5d binary metal oxide, OsIrO₂ binds the terminal O atom most strongly, followed by the 4d-5d binary metal oxide, RuIrO₂ and the 4d-4d metal oxides, *i.e.* RuO₂ and RuRhO₂. The 4d-3d binary metal oxides, RuNiO₂ and RuCoO₂ bind the terminal O atom most weakly. This trend shows that the terminal O atom binding strength as measured by $\delta G(O)$ is rather sensitive to the doping and thus provides the opportunity for optimizing the OER activity.

It should be mentioned that the 1 ML O covered surface with all exposed five-fold metal cationic sites being terminated by O atoms has been identified to be the active site for H₂O splitting on the pure RuO₂(110) surface above 1.23 V.¹² In this work, we did not make attempts to explore all the possible phases, for instance, to consider the possibility of having an extra H on the surface (as surface OH): on RuO₂ (110) the presence of a finite coverage of H on the bridging O atoms at the low overpotential (from 1.23 to 1.58 V) is thermodynamically favored according to the computed surface phase diagram. Although the presence of such species *e.g.* neighboring H, may influence (decrease) the activity, here we only focus on the fully-O covered surface, which may serve as a first and simple model to screen as many as possible surfaces to identify the new OER catalysts.

We then investigated H₂O dissociation kinetics on the 1 ML O-covered surfaces. Our previous work for OER on RuO₂ (110) shows that the first step of H₂O activation in OER, *i.e.* H-O bond dissociation of H₂O on the terminal O, is the rate-determining step.¹² Thus, here we utilize the kinetics of the first step H₂O splitting as a simple tool for assessing the activity of the rutile-type binary metal oxide catalysts without exploring all the likely pathways on different surfaces. This assumes that the rate-determining step remains the first H₂O dissociation

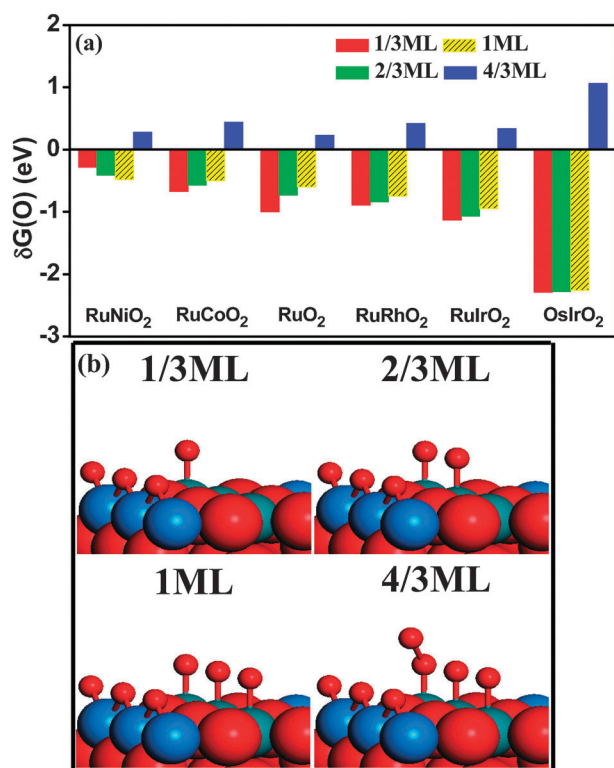


Fig. 2 (a) The differential adsorption energy of the O atom ($\delta G(O)$, eqn (1)) on the (110) surface of six different rutile oxides. Four different O coverages have been considered, ranging from 1/3 ML to 4/3 ML. (b) The structure of the rutile surface at different oxygen coverages (indicated in the figure).

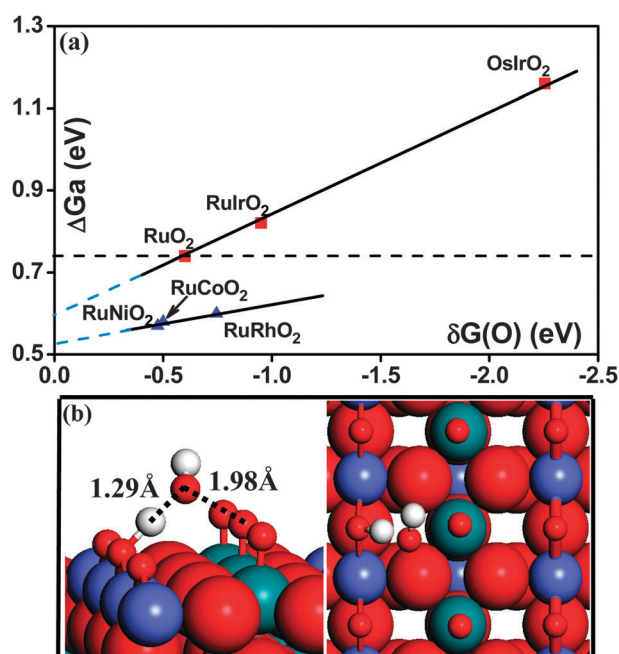


Fig. 3 (a) The plot between $\delta G(O)$ and the free energy barrier of water splitting on the rutile oxides. (b) The optimized TS geometry of OER on the 1 ML O-covered RuCoO_2 (110).

step on these binary oxides, which is reasonable considering that the structure of these rutile-type binary metal oxides is similar to that of RuO_2 . It might be mentioned that we did not take into account the van der Waals energy for H_2O interaction with the oxides, because the van der Waals interactions are generally small (< 0.1 eV)^{36,37} and the main focus of this work is on the trend of OER over different oxide surfaces.

On the 1 ML O-covered surface, we first calculated the reaction barriers of a single H_2O molecule dissociation on the O-covered surface and the TSs have been identified. At the TS, the dissociating H_2O passes its H to the bridging O atom on the surface, while the OH attaches to the terminal O, yielding a OOH species (see Fig. 3). As the dissociating H_2O comes from solution to react with the surface O atoms, *i.e.* the reaction following an Eley–Rideal mechanism, it is a must to take into account the cost of solvation energy and entropy ($\Delta G_{\text{solv}+\text{TS}}$) from the initial state (IS) to the TS under a realistic solid–liquid environment. The free energy barrier (ΔG_a) is then deduced by using a constant $\Delta G_{\text{solv}+\text{TS}}$ value previously calculated on the RuO_2 (*i.e.* 0.54 eV) surface¹² (by combining DFT with periodic continuum solvation model based on modified Poisson–Boltzmann electrostatics and also including the first shell explicit water layer).

We have tentatively plotted $\delta G(O)$ (Fig. 2a) against ΔG_a on all the surfaces in Fig. 3. In general, we found that the higher the $\delta G(O)$ is, the higher ΔG_a will be for the dissociation of H_2O . This is not surprising because the more stable the terminal O is (more negative $\delta G(O)$), the less bonding ability it has to further react with the coming H_2O molecule. On the other hand, it is interesting to notice that these six points cannot be fitted into one single line, indicating that one parameter alone cannot fully describe the H_2O dissociation kinetics even on these structurally similar oxide surfaces.

Specifically, we can classify RuO_2 , RuIrO_2 and OsIrO_2 as one group and RuNiO_2 , RuCoO_2 and RuRhO_2 as another group. The latter group has a lower barrier compared to the former group at the same $\delta G(O)$. This suggests that a second parameter exists and can be utilized to further tune the OER activity. It should be mentioned that we have also calculated the barriers for Ni and Co-involved systems by utilizing the GGA + U functional. We found that the effect of the plus-U is generally small: the barrier difference is 0.02 eV and 0.09 eV for RuNiO_2 and RuCoO_2 , respectively.

We also investigated the H_2O dissociation at the surface coverage more than 1 ML O atoms. In general, we found that H_2O dissociation barrier increases at the higher O coverage conditions. For example, on the RuRhO_2 surface, at the 1 ML O-covered surface, the H_2O dissociation free energy barrier is 0.60 eV, while at the 4/3 ML O-covered surface, the barrier increases to 0.72 eV. While the high O coverage (above 1 ML) is thermodynamically likely at the high potentials (*e.g.* 1.5 V, see Fig. 2), H_2O dissociation kinetics in fact prevent the accumulation of O atoms more than 1 ML: H_2O dissociation becomes slower than O_2 desorption at a coverage above 1 ML and OER can only reach the steady state condition on the 1 ML O covered surface. It is therefore concluded that 1 ML O coverage on these rutile oxide surfaces is the active site for OER even at relative high potentials.

4. Analyses and discussion

Since $\delta G(O)$ alone cannot fully determine the OER activity, it is interesting to ask what else is also important to activity. By closely examining the TS of H_2O dissociation (shown in Fig. 3b), where the dissociating H_2O not only interact with the terminal O but also the bridging O of rutile oxides, we expect that the surface bridging O of oxides may also affect the OER activity. Therefore, it is essential to analyze the difference in the electronic structure of the bridging O between the oxides.

To this end, we calculated the total density of states projected onto the 2p orbitals (p-PDOS) of the bridging O of the oxides. As a representative, we have plotted the bridging O p-PDOS of RuO_2 , RuIrO_2 (the first group), RuNiO_2 and RuCoO_2 (the second group) in Fig. 4. We found that the p-PDOSs look rather similar in the same group, but become different on going from one group to the other. For the bridging O in the first group, there is a significant distribution of O 2p states at low energies, *i.e.* below -5 eV and the major bonding peak appears at -3 eV. On the other hand, the bonding states for the bridging O in the second group are not so obvious, dispersing from -4 to -2 eV. Nevertheless, the bridging O atom in all oxides exhibit non-bonding characteristics with high p-PDOS populations around the Fermi level, apparently due to their lower coordination compared to the bulk O atoms. This is consistent with the identified reaction pattern, that is, the bridging O can accept the H from the dissociating H_2O .

According to the p-PDOS, we can quantitatively compare the relative stability of the bridging O between oxides. We have utilized the eqn (2) to compute the p-band energy (ϵ_p), which is a measure of the activity of the O 2p states in the system. The larger the value is (closer to the Fermi level), the higher activity of the O 2p states would be. The calculated

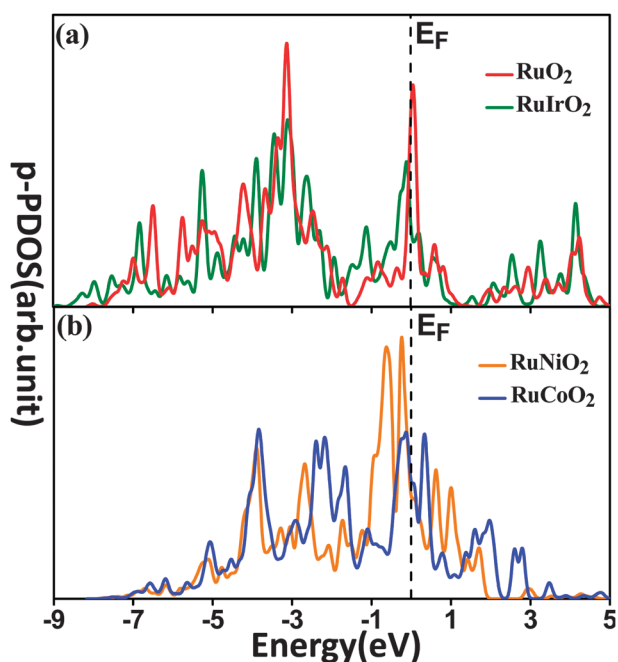


Fig. 4 The density of states projected onto 2p states of the surface bridging O. (a) RuO₂ and RuIrO₂; and (b) RuNiO₂ and RuCoO₂.

ε_p values are -2.16 eV, -2.52 eV, -3.22 eV and -3.37 eV for RuNiO₂, RuCoO₂, RuO₂ and RuIrO₂ oxides, respectively. This trend agrees with the observed OER activity difference between the first and the second group oxides. The difference in the electronic structure of the bridging O is an important factor causing that the first group oxides, represented by RuO₂, RuIrO₂, has a lower activity compared to the second group oxides, represented by RuNiO₂ and RuCoO₂. We can therefore conclude that the bridging O that accepts H during H₂O dissociation also contributes to the OER activity.

$$\varepsilon_p = \frac{\int_{-\infty}^{E_F} \rho \varepsilon d\varepsilon}{\int_{-\infty}^{E_F} \rho d\varepsilon} \quad (2)$$

Finally, it is of interest to estimate the rate of the OER according to the calculated ΔG_a and compare them with those obtained from experiment.¹⁰ The reaction rate is calculated using eqn (3),

$$j = nFN_A^{-1}A \frac{\theta}{S} \exp\left(\frac{-\Delta G_a}{RT}\right) \quad (3)$$

where n is the number of transferring electrons of the elementary step; A is the preexponential factor (it is set as 10^{13}); θ is the coverage of active sites on the surface (for the 1 ML O covered surface, θ is 1 and for the 4/3 ML O covered surface, θ is 2/3); S is the surface area. The equation has been utilized previously for estimating the OER rate on RuO₂.¹² We have plotted the calculated $\log(j)$ against $\delta G(O)$ in Fig. 5, which exhibits a typical “volcano curve”.

It is interesting to compare our calculated rate (current) data with those reported in experiment. The Strasser group¹⁰ has utilized an electrochemical multielectrode cell to search for potential OER catalysts. Among seven binary metal oxides tested that were synthesized by mixing metal precursor in

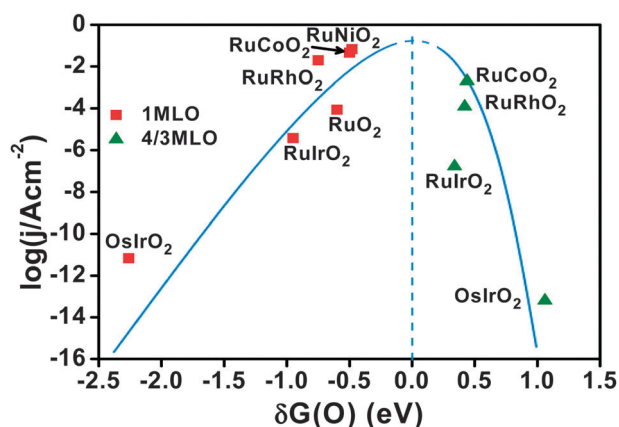


Fig. 5 The calculated reaction rate of OER on different oxides as a function of $\delta G(O)$. The red squares represent the OER on 1 ML O-covered surfaces, and the green triangles represent the OER on 4/3 ML O-covered surfaces.

solution followed by reduction and annealing at 800 °C, the Ru/Co binary system exhibits the highest activity with a 60/40 to 40/60 mole ratio. The rate is about 1.5 times that of Ru/Co(90/10) in Ru/Co(50/50) at 1.55 V. Although the exact structure of Ru/Co mixed oxides remains unknown, our theoretical data also show that RuCoO₂ is more active than RuO₂. The difference between theory and experiment in the rate enhancement may be attributed to the difference in the surface structure considering that an ideal rutile structure is assumed here by taking simply Co as an electronic structure modifier to RuO₂. In addition, Lyons and Floquet group³⁸ prepared Ru_{0.5}Ir_{0.5}O₂ mixed oxide and tested its OER activity in acid solution. According to the measured Tafel line, they showed that the rate on RuO₂ is about 3 times larger than that on Ru_{0.5}Ir_{0.5}O₂ at 1.23 V. From our work, the doping of Ir into RuO₂ will indeed reduce the activity.

From the volcano curve, one can also predict that the most active catalyst for OER emerges when $\delta G(O)$ approaches to zero, suggesting that the presence of weakly adsorbed terminal O atoms is the key for achieving high OER activity. RuNiO₂ and RuCoO₂ are already close to the highest activity in this volcano curve because both oxides have highly active bridging O atoms in addition to the presence of weakly adsorbed terminal O atoms. However, the most active catalyst is not necessarily the best catalyst and many other issues must be considered in practice. One important concern is whether these active rutile-type binary metal oxides are stable enough under realistic conditions, and if not, what the most stable surface structures are. Certainly, this is a challenging topic in theory, involving the search of the global minimum under the realistic conditions and it is beyond the scope of the current work.

Nevertheless, we also tentatively examined the bridging O atom binding energy on the RuNiO₂ and RuCoO₂ at the 1 ML O-covered surface, which are 0.29 eV and -0.42 eV with respect to molecular O₂ at the standard state. These values are significantly smaller compared to those of RuO₂ (-2.37 eV) and RuIrO₂ (-2.45 eV), suggesting that while the doping of Ni and Co can increase the OER activity it is at the expense of the catalyst stability. Since the binding energy of the bridging O is positive (less stable than O₂), the presence of RuNiO₂ as rutile

(1 ML O) at the high potentials is highly questionable. This provides an important hint for catalyst design that on approaching to the top of volcano curve (the terminal O becomes increasingly unstable) the whole catalyst may become unstable with the lattice O atom starting to desorb. A good OER catalyst should therefore achieve the balance between a high activity and a long-term stability. Based on our results, Ru–Co mixed oxides can be a potential building block for practical OER catalysts with good activity and stability. The Co can be an efficient electronic structure modifier to RuO₂ that helps to create more reactive lattice O.

5. Conclusions

This work represents a theoretical attempt to search for the active OER electrocatalysts based on first principles calculations. Five different rutile-type binary metal oxides, namely, RuNiO₂, RuCoO₂, RuRhO₂, RuIrO₂ and OsIrO₂ are investigated and their OER activities are assessed based on a simplified theoretical model. To allow for a fast screening of potential working catalyst, two key properties relevant to OER activity are focused on in this work to assess the performance of different catalysts, (i) the surface O coverage at the concerned potentials and (ii), the H₂O activation kinetics on the O-covered surfaces. The former property reflects the thermodynamic tendency of the surface in holding O atoms at the elevated electrochemical conditions, which dictates the most likely active surface site during OER. The second property is associated with the kinetics of the catalyst in catalyzing OER, in which the first step in H₂O activation is known to be the rate-determining step.

We found that on all the rutile-type binary metal oxide surfaces, the relevant O coverage (above 1.23 V) on the surface is 1 ML, with all the five-fold metal cation sites being terminated by O atoms. On the 1 ML O covered surface, the calculated $\delta G(O)$ is -0.48 , -0.50 , -0.60 , -0.75 , -0.95 and -2.26 eV on the RuNiO₂, RuCoO₂, RuO₂, RuRhO₂, RuIrO₂ and OsIrO₂ surfaces, respectively. The terminal O atom bonds most strongly on OsIrO₂, and has the similar bonding strength on RuO₂, RuCoO₂ and RuNiO₂.

For the first step in H₂O splitting, the calculated free energy barrier is 0.57, 0.58, 0.74, 0.60, 0.82 and 1.16 eV on the RuNiO₂, RuCoO₂, RuO₂, RuRhO₂, RuIrO₂ and OsIrO₂ surfaces, respectively. By plotting the barrier against the differential adsorption energy of the terminal O atom, we found that the barriers for the group RuNiO₂, RuCoO₂ and RuRhO₂ are obviously lower than the other oxides group including RuO₂, RuIrO₂ and OsIrO₂. Fundamentally, we find that in addition to the terminal O on surface, the lattice bridging O also plays an important role in affecting the OER activity. The presence of the active bridging O atoms can help to reduce the H₂O dissociation barrier.

Acknowledgements

This work is supported by National Nature Science Foundation of China (20825311, 21173051, 21103110), 973 program (2011CB808500), Science and Technology Commission of Shanghai Municipality (08DZ2270500) and Program for Professor of Special Appointment (Eastern Scholar) at Shanghai Institute of Higher Learning.

Notes and references

- H. Y. Jung, S. Park and B. N. Popov, *J. Power Sources*, 2009, **191**, 357.
- E. B. Castro, C. A. Gervasi and J. R. Vilche, *J. Appl. Electrochem.*, 1998, **28**, 835.
- R. Kotz, H. J. Lewerenz, P. Bruesch and S. Stucki, *J. Electroanal. Chem.*, 1983, **150**, 209.
- M. E. G. Lyons and M. P. Brandon, *J. Electroanal. Chem.*, 2010, **641**, 119.
- K. Macounova, M. Makarova and P. Krtil, *Electrochem. Commun.*, 2009, **11**, 1865.
- D. E. Hall, *J. Electrochem. Soc.*, 1983, **130**, 317.
- J. Rossmeisl, A. Logadottir and J. K. Nørskov, *Chem. Phys.*, 2005, **319**, 178.
- J. Rossmeisl, Z. W. Qu, H. Zhu, G. J. Kroes and J. K. Nørskov, *J. Electroanal. Chem.*, 2007, **607**, 83.
- H. Dau, C. Limberg, T. Reier, M. Risch, S. Roggan and P. Strasser, *ChemCatChem*, 2010, **2**, 724.
- R. Forgie, G. Bugosh, K. C. Neyerlin, Z. C. Liu and P. Strasser, *Electrochem. Solid-State Lett.*, 2010, **13**, D36.
- S. M. Lin and T. C. Wen, *J. Electrochem. Soc.*, 1993, **140**, 2265.
- Y. H. Fang and Z. P. Liu, *J. Am. Chem. Soc.*, 2010, **132**, 18214.
- K. Macounova, J. Jirkovsky, M. V. Makarova, J. Franc and P. Krtil, *J. Solid State Electrochem.*, 2009, **13**, 959.
- P. D. Tran, V. Artero and M. Fontecave, *Energy Environ. Sci.*, 2010, **3**, 727.
- H. J. Wu, Q. Ruan, B. H. Wang and S. Z. Liu, *Rare. Metal. Mat. Eng.*, 2010, **39**, 1111.
- Z. H. Liang, Y. F. Sun, C. M. Fan, X. G. Hao and Y. P. Sun, *J. Solution Chem.*, 2009, **38**, 1119.
- K. Domen, K. Maeda and R. Abe, *J. Phys. Chem. C*, 2011, **115**, 3057.
- L. M. Da Silva, J. F. C. Boodts and L. A. De Faria, *Electrochim. Acta*, 2001, **46**, 1369.
- J. Jirkovsky, M. Makarova and P. Krtil, *Electrochem. Commun.*, 2006, **8**, 1417.
- C. C. Hu, C. F. Lee and T. C. Wen, *J. Appl. Electrochem.*, 1996, **26**, 72.
- K. C. Fernandes, L. M. Da Silva, J. F. C. Boodts and L. A. De Faria, *Electrochim. Acta*, 2006, **51**, 2809.
- M. Musiani, F. Furlanetto and R. Bertinello, *J. Electroanal. Chem.*, 1999, **465**, 160.
- R. Bertinello, S. Cattarin, I. Frateur and M. Musiani, *J. Electroanal. Chem.*, 2000, **492**, 145.
- P. Salvador, V. M. Fernandez and C. Gutierrez, *Sol. Energy Mater.*, 1982, **7**, 323.
- K. Macounová, M. Makarova, J. Franc, J. Jirkovský and P. Krtil, *Electrochem. Solid-State Lett.*, 2008, **11**, 27.
- C. Baruffaldi, S. Cattarin and M. Musiani, *Electrochim. Acta*, 2003, **48**, 3921.
- A. Valdes, Z. W. Qu, G. J. Kroes, J. Rossmeisl and J. K. Nørskov, *J. Phys. Chem. C*, 2008, **112**, 9872.
- I. C. Man, H. Y. Su, F. Calle-Vallejo, H. A. Hansen, J. I. Martinez, N. G. Inoglu, J. Kitchin, T. F. Jaramillo, J. K. Nørskov and J. Rossmeisl, *ChemCatChem*, 2011, **3**, 1159.
- G. Kresse and J. Furthmüller, *Phys. Rev. B: Condens. Matter*, 1996, **54**, 11169.
- J. P. Perdew, K. Burke and M. Ernzerhof, *Phys. Rev. Lett.*, 1997, **78**, 1396.
- G. F. Wei and Z. P. Liu, *Energy Environ. Sci.*, 2011, **4**, 1268.
- H. F. Wang and Z. P. Liu, *J. Am. Chem. Soc.*, 2008, **130**, 10996.
- C. Shang and Z. P. Liu, *J. Chem. Theory Comput.*, 2010, **6**, 1136.
- V. I. Anisimov, J. Zaanen and O. K. Andersen, *Phys. Rev. B: Condens. Matter*, 1991, **44**, 943.
- Y. H. Fang and Z. P. Liu, *J. Phys. Chem. C*, 2009, **113**, 9765.
- J. Ma, A. Michaelides, D. Alfè, L. Schimka, G. Kresse and E. Wang, *Phys. Rev. B: Condens. Matter Mater. Phys.*, 2011, **84**, 033402.
- J. Carrasco, B. Santra, J. Klimeš and A. Michaelides, *Phys. Rev. Lett.*, 2011, **106**, 026101.
- M. E. G. Lyons and S. Floquet, *Phys. Chem. Chem. Phys.*, 2011, **13**, 5314.